Modeling, Identification and Control, Vol. 44, No. 2, 2023, pp. 43–54, ISSN 1890–1328

Multistage model predictive control with simplified scenario ensembles for robust control of hydropower station

Changhun Jeong [1] Beathe Furenes [2] Roshan Sharma [1]

[1] *Department of Electrical engineering, Information Technology and Cybernetics, University of South-Eastern Norway, Porsgrunn, Norway. E-mail:* changhun.jeong@usn.no / roshan.sharma@usn.no

[2] *Skagerak Kraft AS, Porsgrunn, Norway.*

Abstract

This paper proposes simplification of the scenario ensembles that describe the uncertainty present in a hydropower plant. The simplified scenario tree is further used with a multistage model predictive control for optimal operation of the hydropower station. The proposed method reduces the number of considered scenario ensembles of water inflow forecast into the reservoir in the Dalsfoss hydropower plant, which leads to less computational demand of the multistage MPC. The method takes two steps: the creation of three synthesis scenario ensembles and the estimation of the probability of occurrence of the three synthesis scenario ensembles. The simulation results of multistage MPC with 4 different types of scenario ensembles demonstrate that the proposed simplified method reduces the computation demand of the multistage MPC by 15 times approximately, without degrading its performance.

Keywords: Multistage model predictive control, Uncertainty, Simplified method, Renewable energy

1 Introduction

Hydropower is an attractive renewable energy with two significant benefits; flooding management and energy security. The presence of a reservoir in a hydropower system enables it to hold the water for generating power or ensure the steady water flow in downstream in the future (IEA, 2021; Torabi Haghighi et al., 2019). However, the operation of a hydropower system is challenging. Some operational constraints and requirements must comply when operating a hydropower system, for ensuring safety in the operation and preventing damage to the ecosystem (NVE, 2021). Furthermore, the presence of uncertainty, such as water inflow to a reservoir, exacerbates the difficulty of the operation of a hydropower system.

The operation of the Dalsfoss hydropower plant is not exceptional for the challenge because there are several operational constraints and requirements posed by NVE(NVE, 2021), and uncertainty of water inflow. Thus, Skagerak Kraft, the operator of the plant, has been considering the implementation of model predictive control (MPC). MPC is an appealing control strategy for a constrained multi-input and multi-output system and optimal operation (Morari and Lee, 1999). It aims to achieve optimal operation and satisfy the posed constraints. MPC computes the optimal control sequence by solving an optimal control problem (OCP) and applies the first element of the sequence to the system (Mayne et al., 2000).

The first attempt of utilizing MPC for the Dalsfoss hydropower plant was made internally in Skagerak Kraft AS. It suggested a system model of the Dalsfoss hydropower system and simulated the deterministic MPC with reference region tracking OCP that aims

doi:10.4173/mic.2023.2.1

to keep the water level in a specific range instead of maximizing it. Then, later, the model and the OCP are used to test the stochastic MPC in (Menchacatorre et al., 2019). However, because of the reference region tracking OCP, it is observed a large amount of water was thrown away through floodgates instead of being used for power generation in the future, despite the constraints on the water level being seldom activated.

To address this issue, the new OCP was formulated in (Jeong et al., 2021). The new objective function was designed to maximize the water level at the reservoir and explicit constraints on the water level bounds were posed. As the result, the water level was maximized during the simulations and the constraint of the maximum water level became activated. However, due to the activation of the constraint, the constraint was not satisfied when uncertainty was realized differently from the predicted value. Later, the newly proposed OCP was tested with various sets of weight parameters for finding preferred operational condition in Jeong and Sharma (2022b).

Uncertainty in the system, such as model mismatch and disturbances, can lead to the failure of the optimal operation and even to potential constraint violations during operation (Birge, 1997; Shapiro et al., 2009). There has been much research to counteract the influence of the uncertainty in the MPC framework (Mesbah, 2016). Firstly, Min-max MPC was introduced in (Campo and Morari, 1987). Min-max calculates the control sequence over a single trajectory that aims to counteract the influence of all possible realizations of uncertainty. In other words, it provides the control input for the worst-case scenario of uncertainty. This approach frequently yields a highly conservative control input, while ensuring the robust satisfaction of constraints. Later, multistage MPC appeared as the solution of the highly conservative solution of Min-max MPC in (Scokaert and Mayne, 1998; Lucia et al., 2013). The uncertain system behavior is described by a discrete-time scenario tree, which accounts for the future evolution of uncertainty. Multistage MPC computes many control trajectories over the scenario tree. The effectiveness and performance of the multistage MPC approach have been demonstrated in various industrial applications(Lucia et al., 2013; Klintberg et al., 2016; Maiworm et al., 2015).

Multistage MPC was effective in counteracting the uncertain water inflow in the operation of the Dalsfoss hydropower plant as well (Jeong and Sharma, 2022a). The 50 scenario ensembles of the water inflow forecast are used as the scenario tree for implementing the multistage MPC. As result, no violation was observed. To reduce the computational time, instead of the whole scenario ensembles, the three synthesis scenario ensembles were created and used for multistage MPC. Although the computational demand was significantly reduced and no violation of constraints was observed, the performance was degraded.

This paper proposes a solution, the simplified method, to compensate for the performance degradation when using the synthesis scenario ensembles to enhance the computation speed of the multistage MPC. The simplified method consists of two stages: (1) Generation of synthesis scenario ensembles and (2) estimation of the probability of each synthesis scenario ensemble. The synthesis scenario ensemble must encapsulate the original scenario ensembles and encompass all realizations of uncertainty. The probabilities add more information on uncertainty in the synthesis scenario ensembles. The implementation of this method significantly reduces the size of the optimization problem, yet does not degrade the performance of the multistage MPC framework. The mentioned advantage of the proposed method is demonstrated through a simulation of the Dalsfoss hydropower station system. The simulations of multistage MPCs with 4 different structures of scenario ensembles of water inflow prediction are performed under the moderate water inflow situation, and the flooding situation.

The organization of this paper is as follows: Section 2 provides overviews of multistage MPC, robust horizon, and open-loop robustness analysis. Section 3 introduces the method to simplify the scenario ensembles. The system model of the Dalsfoss hydropower plant system, its operational constraints, and the formulation of the OCP for multistage MPC are explained in Section 4. The simulation setup and the given data of water inflow forecasts and power production plan for running the simulations are described in Section 5. Section 6 presents the simulation results, and the conclusion is discussed in Section 7.

2 Preliminary

2.1 Multistage model predictive control

In a multistage MPC framework, the uncertainty, such as model parameters or disturbances, can be represented by a form of a discrete scenario tree as illustrated in Figure 1. The possible evolution of the uncertainty in the future and the corresponding control inputs are described by branches from a node. The control inputs from multistage MPC can counteract the effects of the uncertainties as new information will be available as the future sampling in the setting of the scenario tree (Lucia et al., 2013).

The system can be expressed as:

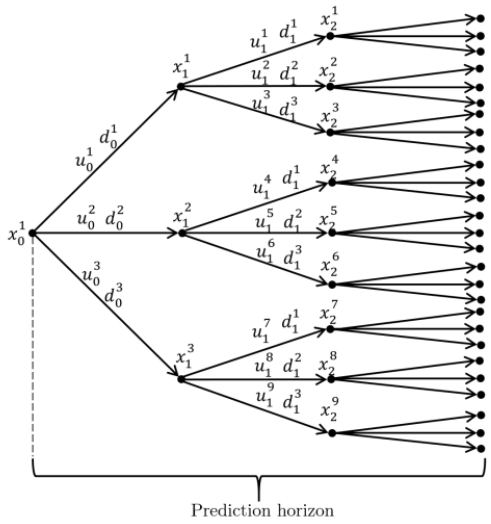

Figure 1: The structure of the scenario tree

$$x_{k+1}^j = f(x_k^{p(j)}, u_k^j, d_k^{r(j)}) \tag{1}$$

where $x_k^{p(j)}$, u_k^j, and $d_k^{r(j)}$ denote the parent state, the control input, and the realization of the uncertainty at time sample k.

It is possible to formulate OCP for multistage MPC as:

$$\begin{aligned}
\underset{u_k^j, \forall (j,k) \in I}{\text{minimize}} \quad & \sum_{i=1}^{S} \omega_i \sum_{k=0}^{Np-1} L(x_{k+1}^j, u_k^j) && \text{(2a)}\\
\text{subject to} \quad & x_{k+1}^j = f(x_k^{p(j)}, u_k^j, d_k^{r(j)}), && \text{(2b)}\\
& x_k^j \in \mathbb{X}, && \text{(2c)}\\
& u_k^j \in \mathbb{U}, && \text{(2d)}\\
& u_k^j = u_k^l \quad \text{if} \quad x_k^{p(j)} = x_k^{p(l)} && \text{(2e)}
\end{aligned}$$

Equation (2a) is the cost function which considers a probability of a scenario by ω_i, and where $L(x_{k+1}, u_k)$ is the stage cost and N_p is the prediction horizon. Equation (2b) is the system model. Equations (2c) and (2d) are bounds of states and control inputs. Equation (2e) denotes non-anticipativity constraints that all the control inputs u_k^k on branches from the same parent node $x_k^{p(k)}$ have to be equal. the non-anticipativity constraints are necessary because the control inputs cannot anticipate the realization of the uncertainty in the future (Lucia et al., 2013).

When implementing multistage MPC, the biggest challenge is to solve the OCP in a reasonable time. It is because of the large size of OCP. The size of the OCP grows exponentially with the prediction horizon and with the number of uncertainties and the number of branches in the scenario tree (Lucia et al., 2013).

2.2 Robust horizon

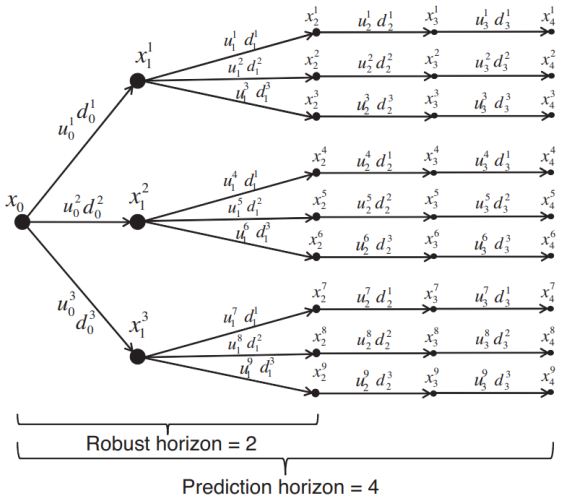

Figure 2: The structure of the scenario tree with a robust horizon

It is critical to have a proper size of OCP by designing the scenario tree properly when running the multistage MPC. One method to avoid the exponential growth of the scenario tree is to utilize a robust horizon. It considers the evolution of the uncertainty up to certain time steps and assumes that the uncertainty remains constant until the end of the prediction horizon, as depicted in Figure 2 (Lucia et al., 2013).

2.3 Open-loop robustness analysis

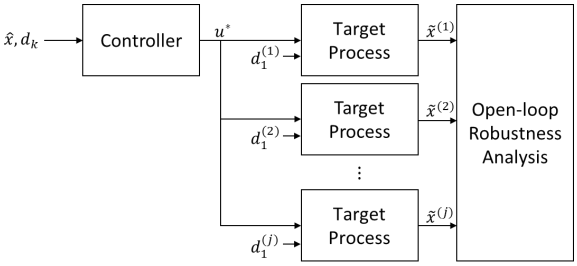

Figure 3: The procedure of open-loop robustness analysis

The open-loop robustness analysis aims to check the constraint violations due to the occurrence of uncertainties in the process. The analysis procedure is illustrated in Figure 3. Once the MPC controller computes

the control inputs, the first element of the control inputs is applied to the model with all possible uncertainties in parallel, and the violation of the constraints is accessed (Jeong et al., 2021).

3 Simplification of scenario ensembles

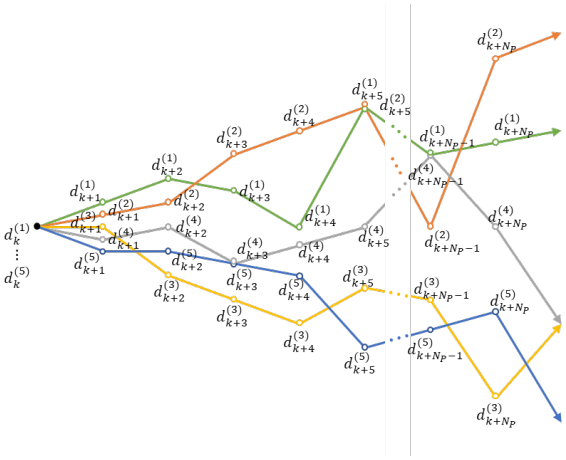

Figure 4: An example of scenario ensembles of uncertainty

The scenario ensembles consist of a collection of distinct scenarios of unpredictability. They resemble a scenario tree with a robust horizon of 1 for the hydro power case study, but the values are not assumed to remain constant after branching. Five example scenario ensembles are displayed in Figure 4. Each color represents one scenario in the ensemble of uncertainty. The number of scenario ensembles, S, over the prediction horizon, N_p, at time sample k can be mathematically expressed as follows:

$$\mathbf{d}_k = \begin{pmatrix} \mathbf{d}_k^{(1)} & \cdots & \mathbf{d}_k^{(S)} \\ \vdots & \ddots & \vdots \\ \mathbf{d}_{k+N_p}^{(1)} & \cdots & \mathbf{d}_{k+N_p}^{(S)} \end{pmatrix} \tag{3}$$

The simplified method streamlines the scenario ensembles to three when there are more than three scenario ensembles present. This is achieved through the following two steps:

Step. 1: The process of creating synthetic scenario ensembles, which represent the original ensembles, can be accomplished by using statistical data such as the minimum, mean, and maximum values of the ensembles at each time step throughout the predicted horizon. As an illustration, consider the five scenario ensembles of uncertainty depicted in Figure 4. These

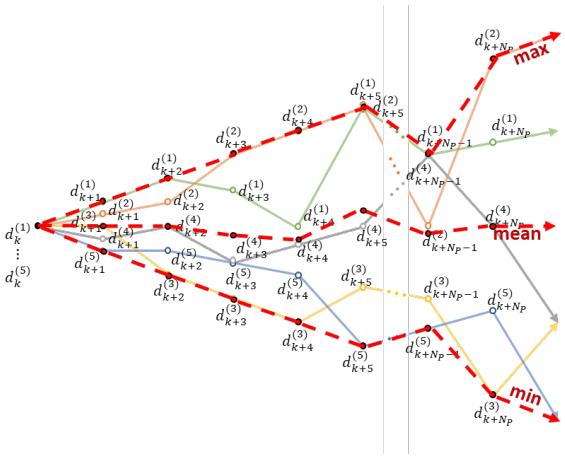

Figure 5: The three synthetic scenario ensembles of the uncertainty from the five example scenario ensembles

ensembles can be transformed into three synthesis scenario ensembles, as demonstrated in Figure 5 with red dotted lines, by using Equation (4),(5), and (6).

$$\mathbf{d}_{\max,k} = \begin{pmatrix} \max(\mathbf{d}_k^{(1)} & \cdots & \mathbf{d}_k^{(S)}) \\ \vdots & \ddots & \vdots \\ \max(\mathbf{d}_{k+N_p}^{(1)} & \cdots & \mathbf{d}_{k+N_p}^{(S)}) \end{pmatrix} \tag{4}$$

$$\mathbf{d}_{\text{mean},k} = \begin{pmatrix} \text{mean}(\mathbf{d}_k^{(1)} & \cdots & \mathbf{d}_k^{(S)}) \\ \vdots & \ddots & \vdots \\ \text{mean}(\mathbf{d}_{k+N_p}^{(1)} & \cdots & \mathbf{d}_{k+N_p}^{(S)}) \end{pmatrix} \tag{5}$$

$$\mathbf{d}_{\min,k} = \begin{pmatrix} \min(\mathbf{d}_k^{(1)} & \cdots & \mathbf{d}_k^{(S)}) \\ \vdots & \ddots & \vdots \\ \min(\mathbf{d}_{k+N_p}^{(1)} & \cdots & \mathbf{d}_{k+N_p}^{(S)}) \end{pmatrix} \tag{6}$$

A simplified scenario ensembles at each time sample k, represented as $\mathbf{d}_{\text{syn},k}$, is constructed as:

$$\mathbf{d}_{\text{syn},k} = \begin{pmatrix} \mathbf{d}_{\max,k} & \mathbf{d}_{\text{mean},k} & \mathbf{d}_{\min,k} \end{pmatrix} \tag{7}$$

The three synthetic scenario ensembles, as described in Equation 7, encompass the full extent of uncertainty represented by the original scenario ensembles in Equation 3.

Step. 2: The use of synthetic scenario ensembles, each with its own probability of occurrence, provides a better representation of uncertainty given by the original scenario ensembles. The probabilities of the three synthetic scenario ensembles are calculated by determining the number of uncertainty points from

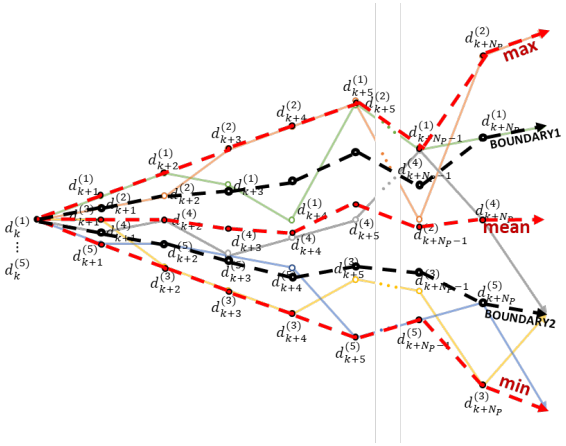

Figure 6: The defined boundary line, when s_1 and s_2 are set as 0.5

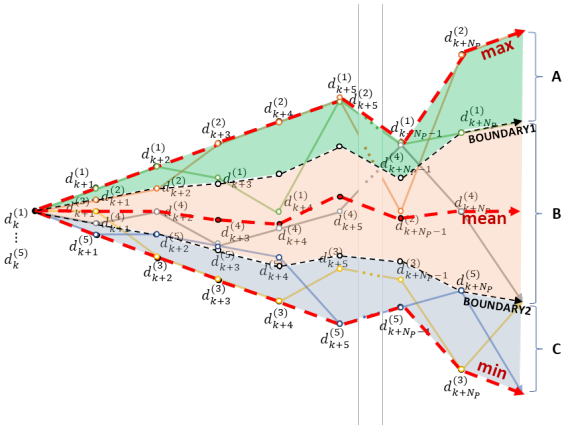

Figure 7: The defined boundary region to calculate the probabilities of occurrences of the synthesis scenario ensembles

the original scenario ensembles that fall within predefined boundary regions. These boundaries can be determined based on either engineering expertise or statistical analysis. For example, the boundaries 1 and 2, denoted by B_1 and B_2, can be established statistically as shown in Figure 6 and are described as follows:

$$B_1 = \mathbf{d}_{\text{mean},k} + s_1 \cdot (\mathbf{d}_{\text{max},k} - \mathbf{d}_{\text{mean},k})$$

$$B_2 = \mathbf{d}_{\text{mean},k} - s_2 \cdot (\mathbf{d}_{\text{mean},k} - \mathbf{d}_{\text{min},k})$$

where s_1 and s_2 are parameters that allow for the adjustment of the boundary ranges. As a result, the boundary regions as depicted in Figure 7 can be represented as follows:

$$\mathbf{A} \in (B_1, \mathbf{d}_{\text{max},k}]$$

$$\mathbf{B} \in [B_1, B_2]$$

$$\mathbf{C} \in [\mathbf{d}_{\text{min},k}, B_2)$$

Regions A, B, and C encompass the probabilities of occurrence for the maximum, mean, and minimum synthetic scenario ensembles, respectively. For instance, the calculation of the probability of occurrence for the maximum synthetic scenario ensemble can be performed as follows:

$$\omega_{\max} = \frac{\sum_{j=1}^{S} \omega_j \cdot N_{\text{A}}^{(j)}}{\sum_{j=1}^{S} \omega_j \cdot N^{(j)}} \tag{8}$$

where ω_j is the possibility of occurence of the j^{th} original scenario ensemble, and $N^{(j)}$ represents the number of uncertainty points in the j^{th} original scenario ensemble, and $N_{\text{A}}^{(j)}$ refers to the number of uncertainty points that belong to region A in the j^{th} original scenario ensemble. The probabilities of occurrence for the mean and minimum synthetic scenario ensembles, ω_{mean} and $\omega_{\min}$, can be calculated in a similar fashion.

3.1 Multistage MPC with simplified scenario ensembles

By utilizing the simplified method, the number of scenario ensembles in the multistage MPC framework is significantly reduced to three. This leads to a substantial decrease in the number of optimization variables by a factor of $\frac{3}{S}$ and also reduces the number of constraints. As a result, the simplified method makes it easier and faster to solve the optimization problem.

4 System description

The Dalsfoss hydropower plant, located in Telemark, Norway along the Kragerø watercourse, consists of a reservoir called Lake Toke and a dam for its power production. Maintaining control over the water level in the reservoir is essential for safe and flexible operation (SkagerakKraft, 2021a,b). However, uncertainty in the water inflow system presents a challenge in controlling the water level. The water inflow to the reservoir is impacted by various factors, such as ice melt, precipitation, and streams. To address this issue, the operation of the Dalsfoss hydropower plant is guided by the forecast which has 50 possible scenario ensembles of water inflow to the reservoir, each with an equal chance of occurrence. These scenarios are generated every 24 hours through the use of complex hydrological models and weather forecast information, providing a 13-day forecast of water inflow into the reservoir.

4.1 System model

A simplified layout of Lake Toke can be seen in Figure 8, which separates the lake into two areas: the

upper region known as Merkebekk, situated on the left side, and the lower region, known as Dalsfoss, located near the dam and hydropower plant on the right side.

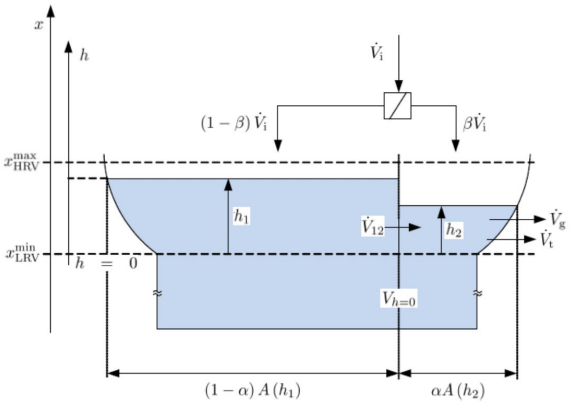

Figure 8: Simplified layout of lake Toke

The water levels in Merkebekk and Dalsfoss, denoted by h_1 and h_2 respectively, act as the states of the system. The flow between the two regions, $\dot{V}_{12}$, is dependent on the difference in water levels. The surface area of Lake Toke, represented as $A(h_i)$, is calculated based on the water level and its unique curvature structure. The fraction of the surface area located in Dalsfoss, denoted by α, must also be considered. The water inflow, $\dot{V}_i$, which comes from various sources such as rivers, precipitation, and ice melting, is described by a coefficient β that represents the ratio of water flowing into Dalsfoss. The operational guidelines must include the consideration of level constraints, such as the minimum low regulated level value (LRV), $x_{\text{LRV}}^{\min}$, and the maximum high regulated level value (HRV), $x_{\text{HRV}}^{\max}$. The flow rates through the floodgate, $\dot{V}_g$, and the turbine, $\dot{V}_t$, combine to make up the total outflow, $\dot{V}_o$, towards the downstream.

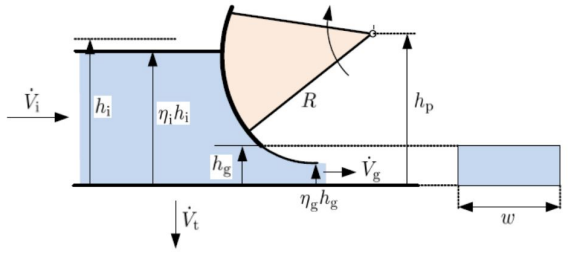

Figure 9: Structure of floodgate

The dynamic model of Lake Toke features two floodgates for regulating the water level within the reservoir, as depicted in Figure 9. The opening heights of these floodgates, represented by h_g, serve as controllable variables that impact the flow rate of water released from the reservoir, $\dot{V}g$. The model is also used in previous works (Menchacatorre et al., 2019; Jeong et al., 2021; Jeong and Sharma, 2022a,b). A summary of the dynamic model, along with its relevant parameters in Table 1, is provided as:

$$\frac{dh_1}{dt} = \frac{1}{(1-\alpha)A(h_1)}((1-\beta)\dot{V}_i - \dot{V}_{12}) \tag{9}$$

$$\frac{dh_2}{dt} = \frac{1}{\alpha A(h_2)}(\beta\dot{V}_i + \dot{V}_{12} - \dot{V}_o) \tag{10}$$

$$A(h_i) = \max(28\times10^6 \cdot 1.1 \cdot h_i^{\frac{1}{10}}, 10^3) \tag{11}$$

$$\dot{V}_{12} = K_{12}\cdot(h_1 - h_2)\sqrt{|h_1 - h_2|} \tag{12}$$

$$\dot{V}_g = C_d \cdot w \cdot \min(h_g, h_2)\sqrt{2g\cdot\max(h_2, 0)} \tag{13}$$

$$\dot{V}_t = a\frac{\dot{W}_e}{x_D - x_q} + b \tag{14}$$

In equation (14), the variable x_q represents the water level at the quay, and it is obtained through the resolution of the following cubic equation.

$$\begin{aligned} 0 = {} & c_1 x_q^3 + (c_2 - c_1 x_D)x_q^2 \\ & + (c_3 - c_2 x_D + c_4\dot{V}_g)x_q \\ & + \dot{W}_e - c_3 x_D - c_4\dot{V}_g x_D - c_5 \end{aligned} \tag{15}$$

The water levels above sea level at Merkebekk, x_M, and Dalsfoss, x_D, are calculated as follows:

$$x_M = h_1 + x_{\text{LRV}}^{\min} \tag{16}$$

$$x_D = h_2 + x_{\text{LRV}}^{\min} \tag{17}$$

4.2 Operational constraints

To ensure safe operation, protect the local wildlife, and prevent damage to nearby properties, the hydropower plant must comply with a set of established constraints:

1. To ensure the safety of individuals and wildlife along the watercourse, it's crucial to avoid abrupt changes in the downstream flow rate, $\dot{V}_o$. Maintaining a consistent flow rate is of utmost importance.

2. To facilitate the free migration of fish and preserve the watercourse, it's vital to maintain the downstream flow rate, $\dot{V}_o$, at a minimum of $4\text{m}^3/\text{s}$.

Table 1: Parameters for Lake Toke model

Parameter	Value	Unit	Comment
α	0.05	-	Fraction of surface area in compartment 2
β	0.02	-	Fraction of inflow to compartment 2
K_{12}	800	$m^{\frac{3}{2}}/s$	Inter compartment flow coefficient
C_d	0.7	-	Discharge coefficient, Dalsfoss gate
w_1	11.6	m	Width of Dalsfoss gate 1
w_2	11.0	m	Width of Dalsfoss gate 2
$x_{\text{LRV}}^{\min}$	55.75	m MSL	Minimal low regulated level value
$x_{\text{HRV}}^{\max}$	60.35	m MSL	Maximal high regulated level value
g	9.81	m/s^2	Acceleration of gravity
a	124.69	Pa^{-1}	Coefficient in equation (14)
b	3.161	m	Coefficient in equation (14)
c_1	0.13152	W/m^{-3}	Polynomial coefficient in (15)
c_2	-9.5241	W/m^2	Polynomial coefficient in (15)
c_3	$1.7234 \cdot 10^2$	W/m	Polynomial coefficient in equation (15)
c_4	$-7.7045 \cdot 10^{-3}$	Pa/m	Polynomial coefficient in equation (15)
c_5	$-8.7359 \cdot 10^{-1}$	W	Polynomial coefficient in equation (15)

3. The water level at Merkebekk must be maintained within specified bounds, as indicated by:

$$x_{\text{M}} \in [x_{\text{LRV}}, x_{\text{HRV}}]$$

These bounds vary based on the season, as outlined in Table. 2.

4. The maximum flow rate through the turbine, $\dot{V}_t$, is capped at $36m^3/s$.

5. The maximum opening height of the floodgates is restricted to 5.6m.

Table 2: Seasonal level requirement

Date	x_{LRV}[m MSL]	x_{HRV}[m MSL]
Jan. 1 - Apr. 30	55.75	60.35
May. 1 - Aug. 30	58.85	59.85
Sept. 1 - Sept. 14	55.75	59.35
Oct. 28 - Nov. 11	55.75	59.85
Nov. 12 - Dec. 31	55.75	60.35

4.3 Optimal control problem

The objective of MPC for the hydropower system is to maximize the utilization of water resources in the generation of electricity, and in satisfying the steady flow and the minimum water flow at downstream. The cost function of the OCP is defined as:

$$J_k = \omega_{x_{\text{M}}} L^2(x_{\text{M},k+i}) + \omega_{\Delta h_g} \Delta h_{g,k}^2 + \omega_{h_g} h_{g,k}^2 + \omega_p p_k^2 \tag{18}$$

The parameters affecting the objective function are listed in Table 3. The first component of the objective function, in Equation (18), aims to maximize the water level at Merkebekk by setting the reference target as the high regulated value (HRV):

$$L(x_k) = x_{\text{M},k} - x_{\text{HRV}} \tag{19}$$

The second term, $\omega_{\Delta h_g} \Delta h_{g,k}^2$, serves to minimize variations in the height of the floodgate opening, thus reducing wear and tear on the floodgate and maintaining a stable flow rate downstream. The third term, $\omega_{h_g} h_{g,k}^2$, aims to minimize the utilization of the floodgate. The final term in the objective function, $\omega_p p^2$, is a penalty term in the event of a violation of the water level constraints. This penalty term allows for a degree of slack from the lower regulated value (x_{LRV}) to prioritize the satisfaction of the minimum flow rate constraint when there is not enough water in the reservoir for both constraints. The slack variable is denoted as p_k. The level constraint is formed as: $x_M \in [x_{LRV} - p, x_{HRV}]$. The value of p_k is determined by solving OCP (Jeong et al., 2021).

Table 3: Parameters for objective function

Parameter	Value	Unit
ω_R	10	-
$\omega_{\Delta u}$	1	-
ω_u	1	-
ω_p	10000	-

Therefore, the optimal control problem for the mul-

tistage MPC is formulated as:

$$\underset{u_k^j, \forall (j,k) \in I}{\text{minimize}} \quad \sum_{i=1}^{S} \omega_i \sum_{k=0}^{Np-1} J_k \tag{20a}$$

$$\text{subject to} \quad x_{k+1}^j = f(x_k^{p(j)}, u_k^j, \dot{V}_{\mathrm{i},k}^{r(j)}, \dot{W}_{\mathrm{e},k}), \tag{20b}$$

$$x_{\mathrm{LRV}} \leq x_{\mathrm{M},k}^j \leq x_{\mathrm{HRV}}, \tag{20c}$$

$$0 \leq u_k^j \leq 5.6m, \tag{20d}$$

$$0 \leq \dot{V}_{\mathrm{t}} \leq 36m^3/s, \tag{20e}$$

$$4m^3/s \leq \dot{V}_{\mathrm{O}} \leq \inf, \tag{20f}$$

$$u_k^j = u_k^l \quad \text{if} \quad x_k^{p(j)} = x_k^{p(l)} \tag{20g}$$

where the system state, x_k^j, is defined as $[h_{1,k}^j, h_{2,k}^j]$, and the control input, u_k^j, is defined as $[h_{\mathrm{g}1,k}^j, h_{\mathrm{g}2,k}^j]$.

5 Simulation setup

5.1 General setting

The simulation period is set for a duration of one month, from April 15th to May 15th. This period includes a significant change in the required water level. The prediction horizon is determined as 13 days (312 hours). The simulations are executed utilizing the IPOPT solver in CasADi (Andersson et al., 2019).

5.2 Uncertainties in the system

The Dalsfoss hydropower plant faces two main sources of uncertainty: the water inflow and the power production plan. To simulate the system more realistically, historical data on power production and the stored scenario ensembles of the water inflow prediction from the real hydropower plant are utilized. A perfect prediction is assumed on the power production plan.

5.2.1 Power production plan

The power production plan for the period of April 15th to May 15th, 2020 is depicted in Figure 10. The data for this plan is obtained from Skagerak Kraft who is the operator of the hydropower plant..

5.2.2 Water inflow forecast

The water inflow forecast is obtained by updating it every 24 hours in the form of 50 scenario ensembles for the next 13 days (312 hours). The 50 scenario ensembles, which were obtained on April 15th, 2020 from Skagerak Kraft, are graphically represented as an example in Figure 11. These ensembles are mathematically represented in a matrix form as follows:

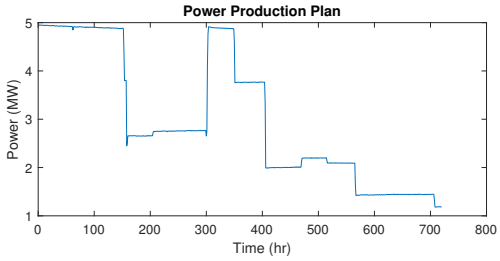

Figure 10: Actual power production history from April 15th, 2020 to May 15th, 2020

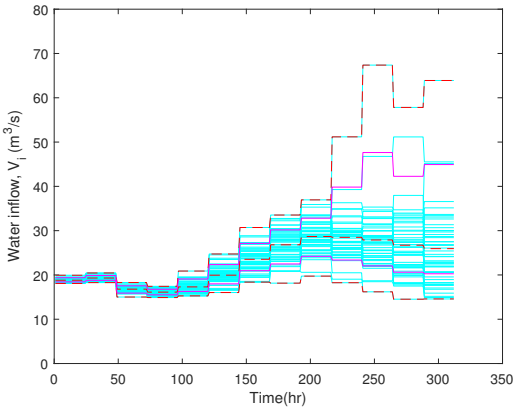

Figure 11: Example of the water inflow forecast obtained on April 15th, 2020 from Skagerak. The cyan color lines are the original 50 scenario ensembles, the red dotted lines represent the three synthesis scenario ensembles, and the pink lines are boundaries with s_1 and s_2 set as 0.5.

$$\dot{V}_{\mathrm{i},k} = f \cdot \begin{pmatrix} \dot{V}_{\mathrm{i},k}^{(1)} & \dot{V}_{\mathrm{i},k}^{(2)} & \cdots & \dot{V}_{\mathrm{i},k}^{(50)} \\ \dot{V}_{\mathrm{i},k+1}^{(1)} & \dot{V}_{\mathrm{i},k+1}^{(2)} & \cdots & \dot{V}_{\mathrm{i},k+1}^{(50)} \\ \vdots & \vdots & \ddots & \vdots \\ \dot{V}_{\mathrm{i},k+312}^{(1)} & \dot{V}_{\mathrm{i},k+312}^{(2)} & \cdots & \dot{V}_{\mathrm{i},k+312}^{(50)} \end{pmatrix}, \tag{21}$$

Where the columns in the matrix represent individual water inflow scenarios. The severity of flooding conditions is described through the use of a flooding coefficient, f, which is set to values of 1 and 2 to represent the moderate water inflow situation and the flooding situation, respectively. For an example, with f = 2, the original real water inflow ensembles are all multiplied by 2 to represent a flood situation.

In this paper, the scenario ensembles of the water inflow prediction are chosen for implementing multistage MPC with notations as described below:

- **MS** contains the original 50 scenario ensembles of the water inflow forecast without any simplification.

- **OS** has the original three scenario ensembles of the water inflow forecast. They are ensembles that have maximum, median, and minimum accumulated amounts of water inflow over the forecast period among all ensembles. The scenario ensemble numbers i, l, and m are chosen as:

$$\sum \dot{V}^{(i)}_{\mathrm{i},k} = \max(\sum \dot{V}^{(1)}_{\mathrm{i},k}, \sum \dot{V}^{(2)}_{\mathrm{i},k}, \ldots, \sum \dot{V}^{(50)}_{\mathrm{i},k})$$

$$\sum \dot{V}^{(l)}_{\mathrm{i},k} = \mathrm{median}(\sum \dot{V}^{(1)}_{\mathrm{i},k}, \sum \dot{V}^{(2)}_{\mathrm{i},k}, \ldots, \sum \dot{V}^{(50)}_{\mathrm{i},k})$$

$$\sum \dot{V}^{(m)}_{\mathrm{i},k} = \min(\sum \dot{V}^{(1)}_{\mathrm{i},k}, \sum \dot{V}^{(2)}_{\mathrm{i},k}, \ldots, \sum \dot{V}^{(50)}_{\mathrm{i},k})$$

  where

$$\sum \dot{V}^{(j)}_{\mathrm{i},k} = \dot{V}^{(j)}_{\mathrm{i},k+1} + \dot{V}^{(j)}_{\mathrm{i},k+2} + \cdots + \dot{V}^{(j)}_{\mathrm{i},k+312}$$

- **Syn(p)** contains three synthetic scenario ensembles with probability distribution information, which is the proposed method in this paper. To set boundary, values of s_1 and s_2 are set as 0.5.

- **Syn(e)** has three synthetic scenario ensembles with equal probability. The synthetic scenario ensembles are constructed by applying the first step of the simplification, Equations (4), (5), and (6). Then, the equal probability is given to the scenario ensembles without using the second step of the simplification.

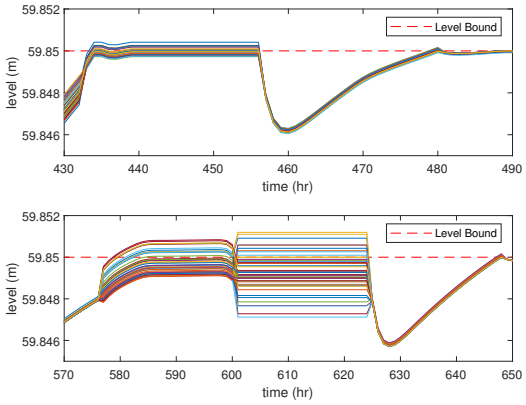

Figure 12: The potential constraint violations caused by implementing multistage MPC using three original scenarios (OS)

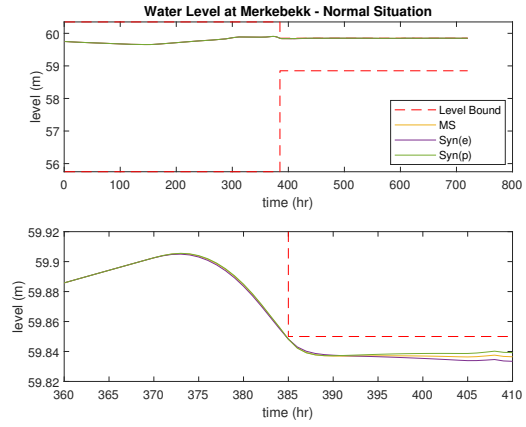

Figure 13: The water level at Merkebekk during the simulation under the moderate water inflow situation

6 Result

6.1 Open-loop Robustness anaylsis

Multistage MPCs with **MS**, **Syn(e)**, and **Syn(p)** show good robustness against constraint violations caused by water inflow uncertainty. This is not the case for multistage MPC with **OS**, as demonstrated by simulations that reveal potential constraint violations (depicted in Figure 12). The figure illustrates possible water level trajectories at Merkebekk from the open-loop robustness analysis, with each line representing a distinct scenario. The analysis shows that under the moderate water inflow situation, there are 283 potential violations, and this number increases to 567 in the flooding situation. As multistage MPC with **OS** is not robust to constraint violations, the simulation results from this method will not be discussed further in this paper.

6.2 Simulation result

The simulation results of the water level at Merkebekk under the moderate water inflow situation ($f = 1$) are presented in Figure 13. The upper plot of the figure provides an overview of the water level through the entire simulation period, while the lower plot provides a closer examination of the water level during the sharp fluctuations in the level bounds.

The simulation results of the flooding situation ($f = 2$) are presented in Figure 14. The topmost plot in this figure illustrates the variation of the water level at Merkebekk over the entire simulation duration. The two lower plots in the figure serve to provide a more detailed view of the water level changes during selected periods, effectively being the magnified sections of the topmost plot.

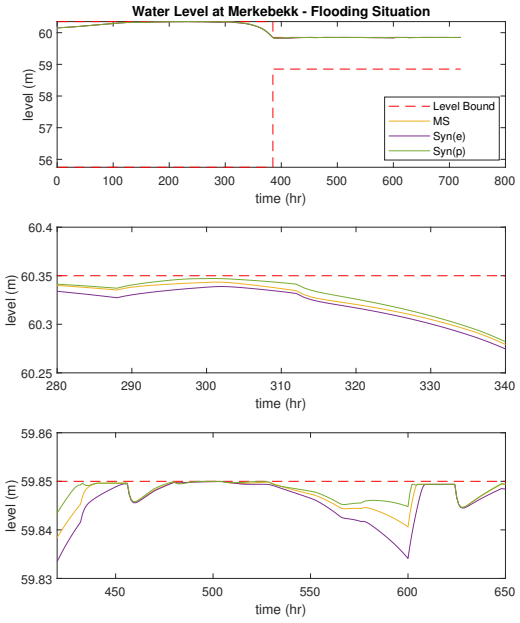

Figure 14: The water level at Merkebekk during the simulation under the flooding situation

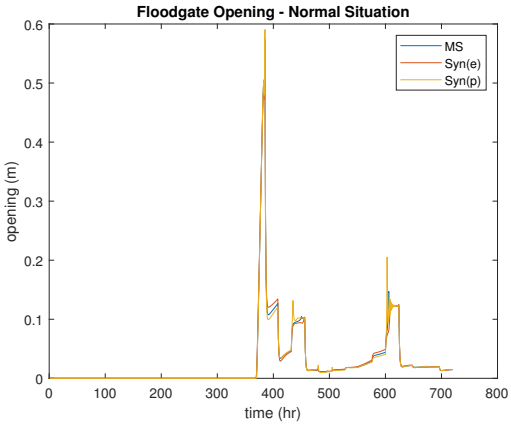

Figure 15: Floodgate opening height through simulations in moderate water inflow situation

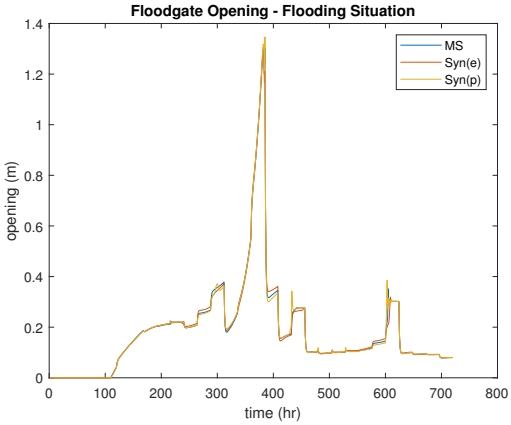

Figure 16: Floodgate opening height through simulations in flooding water inflow situation

The representation of the water level changes in both Figure 13 and Figure 14 are depicted by several lines, each of which corresponds to different simulation scenarios. The red dotted lines indicate the boundaries of the level constraints, represented by x_{LRV} and x_{HRV}. The water level simulated by multistage MPC with **MS** is indicated by the yellow line, while the result of the simulation of multistage MPC with **Syn(e)** is depicted by the purple line. The green line represents the water level changes simulated by multistage MPC with **Syn(p)**.

The opening heights of one floodgate gate with different multistage MPCs(with **MS**, **Syn(e)**, and **Syn(p)**) during the simulation are depicted in Figures 15 and 16. The opening heights of the other floodgate are almost identical to the illustrated figures. Figure 15 represents the opening height of the floodgate under the moderate water inflow situation. Figure 16 presents the opening height of the floodgate during the flooding situation. The opening heights of the floodgate, are indicated by yellow, purple, and green lines, corresponding to the results generated by multistage MPCs with **MS**, **Syn(e)**, and **Syn(p)**, respectively.

Under the moderate water inflow situation, the water level constraints are rarely activated, as the amount of water flowing into the reservoir is not large. Therefore, three multistage MPCs with **MS**, **Syn(e)**, and **Syn(p)** control the system almost identically. During the early stages of the simulation, until around 370 hours, the water levels are controlled by all MPC types and remain relatively unchanged as shown in the upper plot of Figure 13. This period, seen in the left half of the upper plot in Figures 15 and 16, exhibits no significant control actions. However, when the level constraint change, the floodgates start opening, from around 360 hours, to ensure the water level does not exceed the constraint. After 395 hours, subtle differences in the water levels are observed for each multistage MPC, with the highest water level being demonstrated by multistage MPC with **Syn(p)**, the middle water level by multistage MPC with **MS**, and the lowest water level by multistage MPC with **Syn(e)**.

For the flooding situation, the inflow of water into the reservoir is much larger, resulting in a rapid in-

crease in the water level. No control action is taken on the floodgates until 100 hours because the water level does not reach the maximum water level as depicted in Figure 16. As soon as the water level reaches the maximum level, the floodgates are opened to maintain the water level within the constraints. All of the multistage MPCs effectively manage to maintain the water level while satisfying all constraints, but there are slight differences in the water levels among the different multistage MPCs. In line with the simulation result of the moderate water inflow situation, multistage MPC with **Syn(p)** has the highest water level, multistage MPC with **MS** has the middle water level, and multistage MPC with **Syn(e)** has the lowest water level in the flooding scenario.

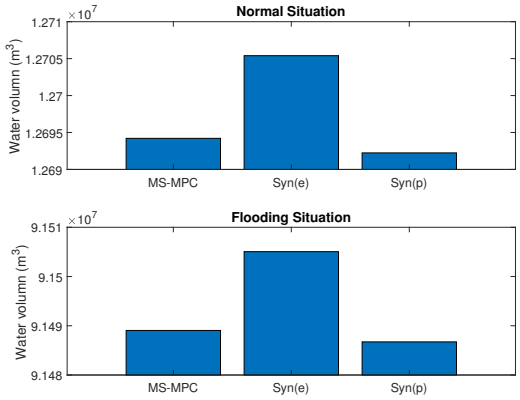

Figure 17: The total amount of water thrown out through floodgates during the simulation period

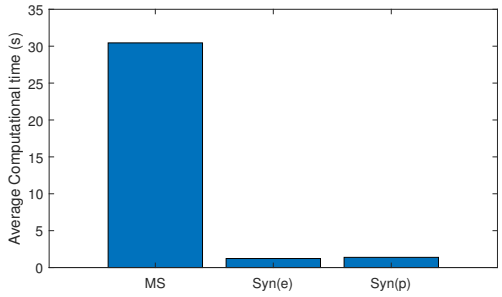

Figure 18: Average computation time for optimization on each time sample

Figure 17 illustrates the total amount of discharged water through the floodgates during the simulation period. As depicted in the figure, multistage MPC with **Syn(p)** exhibits a slightly lower flow rate compared to multistage MPC with **MS**. On the other hand, multistage MPC with **Syn(e)** displays the highest amount of water discharge through the floodgates over the simulation period.

The computational speed of each multistage MPC is presented in Figure 18. Multistage MPC with **MS** requires the longest computation time, with an average of approximately 30 seconds per time sample. In contrast, multistage MPCs with **Syn(p)** and **Syn(e)** have significantly lower computation time, with an average of approximately 2.5 seconds per time sample.

7 Conclusion

In conclusion, this paper presents a practical and efficient method for simplifying the scenario ensembles for multistage MPC applied to the Dalsfoss hydropower station. By using the proposed method, the size of the OCP was reduced by 94%, and the computational speed for solving the OCP was accelerated by 15 times. The simulation results indicate that the performance of multistage MPC with the simplified method (**Syn(p)**) is better or competitive with multistage MPC without using the simplified method (**MS**), and show the improvement in the performance from multistage MPC with (**Syn(e)**), while satisfying all the level constraints. The proposed method in this paper probably cannot be generalized as the simplification of multistage MPC for all types of processes. However, for processes where the uncertainty is already described by scenario ensembles, the proposed method can be effectively used to make the multistage MPC, which a dynamic optimizer for robust control, much more faster and real time implementable.

References

Andersson, J. A. E., Gillis, J., Horn, G., Rawlings, J. B., and Diehl, M. CasADi – A software framework for nonlinear optimization and optimal control. *Mathematical Programming Computation*, 2019. 11(1):1–36. doi:10.1007/s12532-018-0139-4.

Birge, J. R. State-of-the-art-survey–stochastic programming: Computation and applications. *INFORMS Journal on Computing*, 1997. 9(2):111–133. doi:10.1287/ijoc.9.2.111.

Campo, P. J. and Morari, M. Robust model predictive control. In *1987 American Control Conference*. pages 1021–1026, 1987. doi:10.23919/ACC.1987.4789462.

IEA. Hydropower special market report—analysis and forecast to 2030. https://www.iea.org/reports/

hydropower-special-market-report,License:CCBY4.0, 2021.

Jeong, C., Furenes, B., and Sharma, R. MPC operation with improved optimal control problem at dalsfoss power plant. *Proceedings of SIMS EUROSIM conference 2021*, 2021. 11(1):226–233. doi:10.3384/ecp21185226.

Jeong, C. and Sharma, R. Stochastic mpc for optimal operation of hydropower station under uncertainty. *IFAC PapersOnLine*, 2022a. 55(7):155–160. doi:10.1016/j.ifacol.2022.07.437.

Jeong, C. and Sharma, R. Tuning model predictive control for rigorous operation of the dalsfoss hydropower plant. *Energies (Basel)*, 2022b. 15(22):8678. doi:10.3390/en15228678.

Klintberg, E., Dahl, J., Fredriksson, J., and Gros, S. An improved dual newton strategy for scenario-tree mpc. *2016 IEEE 55th Conference on Decision and Control (CDC)*, 2016. pages 3675–3681. doi:10.1109/CDC.2016.7798822.

Lucia, S., Finkler, T., and Engell, S. Multi-stage nonlinear model predictive control applied to a semi-batch polymerization reactor under uncertainty. *Journal of Process Control*, 2013. 23(9):1306–1319. doi:10.1016/j.jprocont.2013.08.008.

Maiworm, M., Bäthge, T., and Findeisen, R. Scenario-based model predictive control: Recursive feasibility and stability. In *IFAC-PapersOnLine*, volume 48. pages 50–56, 2015. doi:10.1016/j.ifacol.2015.08.156.

Mayne, D., Rawlings, J., Rao, C., and Scokaert, P. Constrained model predictive control: Stability and optimality. *Automatica (Oxford)*, 2000. 36(6):789–814. doi:10.1016/S0005-1098(99)00214-9.

Menchacatorre, I., Sharma, R., Furenes, B., and Lie, B. Flood management of lake toke: Mpc operation under uncertainty. 2019. doi:10.3384/ecp20179.

Mesbah, A. Stochastic model predictive control: An overview and perspectives for future research. *IEEE control systems*, 2016. 36(6):30–44. doi:10.1109/MCS.2016.2602087.

Morari, M. and Lee, J. H. Model predictive control : past, present and future. *Computers chemical engineering*, 1999. 23(4-5):667–682. doi:10.1016/S0098-1354(98)00301-9.

NVE. Supervision of dams, (accessed: 24.05.2021). https://www.nve.no/supervision-of-dams/?ref=mainmenu, 2021.

Scokaert, P. and Mayne, D. Min-max feedback model predictive control for constrained linear systems. *IEEE transactions on automatic control*, 1998. 43(8):1136–1142. doi:10.1109/9.704989.

Shapiro, A., Dentcheva, D., and Ruszczyński, A. *Lectures on stochastic programming: modeling and theory*. MOS-SIAM Series on Optimization. Society for Industrial and Applied Mathematics, 2009.

SkagerakKraft. Dalsfos, (accessed: 24.05.2021). https://www.skagerakkraft.no/dalsfos/category1277.html, 2021a.

SkagerakKraft. Kragerø watercourse system, (accessed: 24.05.2021). https://www.skagerakkraft.no/kragero-watercourse/category2391.html, 2021b.

Torabi Haghighi, A., Ashraf, F. B., Riml, J., Koskela, J., Kløve, B., and Marttila, H. A power market-based operation support model for sub-daily hydropower regulation practices. *Applied Energy*, 2019. 255:113905. doi:https://doi.org/10.1016/j.apenergy.2019.113905.